ACS APPLIED MATERIALS & INTERFACES

Research Article

www.acsami.org

Bioreducible POSS-Cored Star-Shaped Polycation for Efficient Gene Delivery

Yan-Yu Yang,[†,‡] Xing Wang,[‡] Yang Hu,[†] Hao Hu,[†] De-Cheng Wu,[*,‡] and Fu-Jian Xu[*,†]

[†]State Key Laboratory of Chemical Resource Engineering, Key Laboratory of Carbon Fiber and Functional Polymers, Ministry of Education, Beijing Laboratory of Biomedical Materials, College of Materials Science & Engineering, Beijing University of Chemical Technology, Beijing 100029, China

[‡]Beijing National Laboratory for Molecular Sciences, State Key Laboratory of Polymer Physics & Chemistry, Institute of Chemistry, Chinese Academy of Sciences, Beijing 100190, China

Supporting Information

ABSTRACT: The bioreducible star-shaped gene vector (POSS-(SS-PDMAEMA)$_8$) with well-defined structure and relatively narrow molecular weight distribution was synthesized via atom transfer radical polymerization (ATRP) of (2-dimethylamino)ethyl methacrylate (DMAEMA) from a polyhedral oligomeric silsesquioxane (POSS) macroinitiator. POSS-(SS-PDMAEMA)$_8$ was composed of a biocompatible POSS core and eight disulfide-linked PDMAEMA arms, wherein the PDMAEMA chain length could be adjusted by controlling polymerization time. POSS-(SS-PDMAEMA)$_8$ can effectively bind pDNA into uniform nanocomplexes with appropriate particle size and zeta potential. The incorporation of disulfide bridges gave the POSS-(SS-PDMAEMA)$_8$ material facile bioreducibility. In comparison with POSS-(PDMAEMA)$_8$ without disulfide linkage, POSS-(SS-PDMAEMA)$_8$ exhibited much lower cytotoxicity and substantially higher transfection efficiency. The present work would provide useful information for the design of new POSS-based drug/gene carriers.

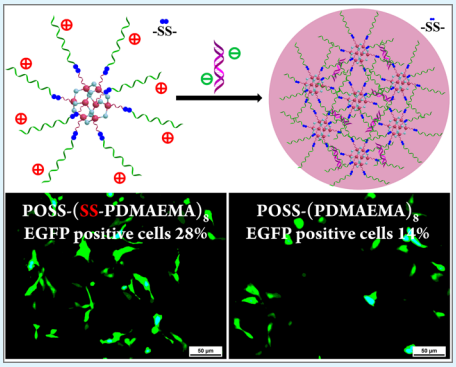

KEYWORDS: *POSS, disulfide bond, bioreducible, vector, gene transfection*

INTRODUCTION

Gene therapy is a very promising strategy to supplement or alter genes within individual cells to treat genetic diseases, cancer, viral infections and cardiovascular disease.[1−3] Gene therapy is constitutive of the delivery of plasmid DNA (pDNA) encoding therapeutic proteins or RNA interference (RNAi), resulting in gene expression or gene silencing. Design and synthesis of nontoxic gene vectors with high transfection efficiency is a most urgent task for gene therapy. Compared with incipient viral vectors and cationic liposomes, polycations, as the developing and dominating type of nonviral gene vectors, have advantages on low host immunogenicity and mass production.[4−6] Polycations condense the negatively charged pDNA into compact nanocomplexes, which can enter cells via endocytosis and be dissociated to release DNA for gene expression.[7] There are different polycations which can be used as gene carriers, such as polyethylenimine (PEI),[8] poly(2-dimethylamino)ethyl methacrylate (PDMAEMA),[9,10] dendrimer polycations,[11,12] hyperbranched poly(amino ester)s,[13] and polysaccharide-based cationic carriers.[14] PDMAEMA is one of the most popular polycations for gene therapy because of relative cytotoxicity and easy preparation.

In general, high-molecular-weight polycations always have high transfection efficiency, but simultaneously suffer from a large damage to cells. On the other hand, low-molecular-weight polycations show much lower cytotoxicity, yet display poor transfection efficiency. Star-shaped polycations with the dense molecular architectures and flexible tailored structure[9,15] were reported to exhibit higher transfection efficiency and lower toxicity than linear counterparts with the same molecular weight.[16,17] Plenty of star-shaped polycations, containing a biocompatible core such as cyclodextrins,[9] glucose,[18] polyphenylene,[19] and polyhedral oligomeric silsesquioxanes (POSS),[20−22] display excellent performance in gene therapy. A typical POSS molecule with a three-dimensional structure of the cage consists of a cubic silica core and eight organic corner groups around outside. The eight corner organic groups can be easily modified into kinds of functional groups, such as amino, thiol, hydroxyl, and halogen. These groups are conveniently used for the preparation of multifunctional polymers with POSS cores.[23,24] In addition, because of good biocompatibility of POSS, POSS-based materials have been used for different biomaterials, such as tissue implants,[25] drug delivery systems.[26] POSS-based materials also can be designed to be gene vectors for gene therapy. Loh and co-workers reported that star-shaped POSS-based PDMAEMA was a better gene vector than linear PDMAEMA.[20] Lu et al prepared POSS-containing star-shaped poly(L-lysine) dendrimers and studied its properties in gene delivery.[22]

Received: October 17, 2013
Accepted: December 3, 2013
Published: December 3, 2013

It is well-known that delivery system with responsivity exhibit outstanding perform in gene and drug delivery.[10,11] Disulfide bonds can be easily cleaved under intracellular condition, so incorporation of disulfide linkage in gene vectors can endow gene delivery system with reducible responsivity.[27,28] Atom transfer radical polymerization (ATRP) is always proposed to prepare well-defined polymers for its well control on polymerization.[29] In the present study, we synthesized a macro-ATRP agent (POSS-$(SS\text{-}Br)_8$) with eight disulfide-linked initiation sites, and then prepared a series of bioreducible star-shaped gene vectors (POSS-$(SS\text{-}PDMAEMA)_8$s) composed of a POSS core and eight disulfide-linked PDMAEMA arms with different molecular weights. The bioreducible POSS-$(SS\text{-}PDMAEMA)_8$s are readily degraded into low-molecular-weight polycations under intracellular condition, and thus higher transfection efficiency and lower toxicity could be obtained. POSS-$(SS\text{-}PDMAEMA)_8$s are promising as new efficient gene vectors for gene therapy.

EXPERIMENTAL SECTION

Materials. Octa-vinyloctasilasesquioxane (V-POSS, 98%) was purchased from Hybrid Plastics (Hattiesburg, MS). Branched polyethylenimine (PEI, 25KDa), cysteamine hydrochloride (99%), 2,2-dimethoxy-2-phenylacetophenone (DMPA, 99%), succinic anhydride (99%), 1-(3-dimethylaminopropyl)-3-ethylcarbodiimide hydrochloride (EDCI, 99%), 4-(dimethylamino)-pyridine (DMAP, 99%), copper(I) bromide (CuBr, 99%), 1,1,4,7,10,10-hexamethyltriethylenetetramine (HMTETA, 99%), penicillin, strep-tomycin 2-(dimethylamino)ethyl methacrylate (DMAEMA, >98%), and 3-(4,5-Dimethylthiazol-2-yl)-2,5-diphenyl tetrazolium bromide (MTT), were obtained from Sigma–Aldrich. DMAEMA was distilled under reduced pressure, and stored at −20 °C. *N,N*-Dimethylformamide (DMF) and dichloromethane (DCM) were deoxygenated and dried by using a commercial solvent purification system (Innovative Technology) before use. 2-Bromo-2-methyl-propionic acid 2-(2-hydroxy-ethyldisulfanyl)-ethyl ester (BIBB-SS−OH) was synthesized via esterification (see the Supporting Information). HepG2 cell lines and COS7 cell lines were obtained from the American type Culture Collection.

Synthesis of Amine-Terminated POSS (A-POSS) and Carboxyl-Terminated POSS (C-POSS). V-POSS (3.18 g, 5 mmol), cysteamine hydrochloride (11.3 g, 0.1 mol) and DMPA (0.42 g, 1.64 mmol) were dissolved in 200 mL of THF/MeOH (v/v, 3/1). The mixture was purged with argon for 15 min and then exposed to the UV irradiation under a 365 nm UV lamp at room temperature for 3 h. A mount of white precipitate was collected by filtration and washed with THF/MeOH (v/v, 5/1) solution for five times. A-POSS was obtained as white power after drying under vacuum (yield: 6.5 g, 84.4%).

For preparation of C-POSS, succinic anhydride (4.5 g, 45.0 mmol) was added to 50 mL of MeOH containing A-POSS (3.95 g, 2.55 mmol) and triethylamine (3 mL, 21.6 mmol). The resultant reaction mixture was stirred at room temperature. After 2 h, chloroform was poured into the reaction solution, and white precipitation was collected via filtration and washed with chloroform. The white powder, C-POSS, was obtained after drying under vacuum (yield: 4.1 g, 78.8%).

Synthesis of POSS-$(SS\text{-}Br)_8$. C-POSS (2.48 g, 1 mmol), DMAP (0.2 g, 1.6 mmol), EDCI (1.92 g, 10 mmol) and anhydrous DMF (30 mL) were added to a two-necked round-bottom flask under an argon atmosphere. Then, a solution of BIBB-SS−OH (3.0 g, 10 mmol) in 10 mL of anhydrous DMF was added dropwise to the above mixture. After 48 h, DMF was evaporated under reduced pressure. Ethyl acetate was added and then the organic phase was washed with 1 M HCl aqueous solution, saturated NaCl aqueous solution and deionized water. The organic phase was dried by anhydrous Na_2SO_4 and followed by condensed. The crude product was purified by precipitating into diethyl ether for three times to remove the excess BIBB-SS−OH. POSS-$(SS\text{-}Br)_8$ was obtained after drying under vacuum (yield: 3.6 g, 85%).

Synthesis of Star-Shaped POSS-$(SS\text{-}PDMAEMA)_8$s via ATRP. The synthesis process of POSS-$(SS\text{-}PDMAEMA)_8$s was conducted under the typical conditions of ATRP. POSS-$(SS\text{-}Br)_8$ (0.1 g, 0.125 equiv), DMAEMA (4 mL, 120 equiv) and HMTETA (54 μL, 1 equiv) were added into a 25 mL flask containing 6 mL of methanol/water (5.9/0.1, v/v). The reaction system was degassed by purging argon for 20 min before adding CuBr (29 mg, 1 equiv) under an argon atmosphere. The flask was purged with argon for another 10 min, and then sealed with a rubber stopper under an argon atmosphere. The polymerization process was conducted under continuous stirring at room temperature from 20 to 40 min. The reaction was stopped by diluting with THF. The THF solution was passed through a short alumina column to remove copper salts. After removal of THF by rotary evaporator, the POSS-$(SS\text{-}PDMAEMA)_8$ residues were precipitated in excess hexane for three times to remove unreacted monomer. Finally, the products were dried under reduced pressure. The yields of POSS-$(SS\text{-}PDMAEMA)_8$ at polymerization time of 20, 30, and 40 min were 0.3, 0.45, and 0.64 g, respectively. The control sample without the disulfide linkages between the POSS core and PDMAEMA arms, POSS-$(PDMAEMA)_8$, was prepared via ATRP by a macroinitiator agent, POSS-Br_8. POSS-Br_8 had a similar structure to POSS-$(SS\text{-}Br)_8$ except the disulfide group. The synthetic process of POSS-$(PDMAEMA)_8$ was illustrated in the Supporting Information.

Characterization of Polymer. Gel permeation chromatography (GPC) and nuclear magnetic resonance (NMR) spectroscopy were utilized to measure the molecular weights and the chemical structure of polymers. GPC measurements of POSS-$(SS\text{-}PDMAEMA)_8$s were carried out on a Waters GPC system equipped with a refractive index detector (Waters-2414) and a dual wavelength (λ) UV detector (Waters-2487) using five Waters Styragel columns. Tetrahydrofuran was used as the eluent at a flow rate of 1 mL/min at 25 °C. Calibration of the molecular weight of polymers was based on polystyrene standards. ^1H and ^{13}C NMR spectra were obtained on a Bruker DRX-400 spectrometer. ^{29}Si NMR spectra were obtained on a Bruker DRX-300 spectrometer. Characterization of Polymer/pDNA Nanocomplexes.

The detailed procedure of making polymer/pDNA nanocomplexes was reported in our earlier work.[30] Plasmid pRL-CMV encoding Renilla luciferase was purchased from Promega Co. (Cergy Pontoise, France). The plasmid DNA (pDNA) was amplified and further purified.[30] 0.5 mg/mL pDNA in tris-EDTA (TE) buffer and polymer solutions with a nitrogen concentration of 10 mM in highly purified water were prepared before every use. Star-shaped polymers to DNA ratios were expressed as molar ratios of nitrogen (N) in the POSS-$(SS\text{-}PDMAEMA)_8$s to phosphate (P) in pDNA (N/P ratios). An average mass weight of 325 per phosphate group of DNA was assumed.[31] All polymer/pDNA nanocomplexes at different N/P ratios were formed by mixing certain volume of polymer solution and pDNA solution homogeneously and further incubated for 30 min at ambient temperature.

Agarose gel electrophoresis was utilized to determine the ability of POSS-$(SS\text{-}PDMAEMA)_8$s to bind the pDNA into NPs. This procedure was detailedly reported in the literature.[30] Gel electrophoresis was implemented in a Sub-Cell system (Bio-Rad Laboratories) and DNA bands were visualized and photographed by a UV transilluminator and BioDco-It imaging system (UVP Inc.). The evaluation assay of heparin-induced release of pDNA from nanocomplexes in vitro was similar to those reported in the literatures.[27,32]

The zeta potentials and particle sizes of the nanocomplexes were determined by a Zetasizer Nano ZS (Malvern). The assay process was described earlier.[30] The atomic force microscopy (AFM) system was applied to observe the morphology of nanocomplexes and AFM images were obtained on a Nanoscope Multimode III AFM instrument (Vecco, USA) in tapping mode.

Cell Viability. The cell viability of polymer/pDNA nanocomplexes at different N/P ratios in HepG2 and COS7 cell lines was determined by MTT assay that is reported in our earlier work.[30] In the final stage, the absorbance was measured using a microplate reader (Spectra Plus, Tecan, Zurich, Switzerland) at a wavelength of 570 nm. The computational method of cell viability (%), relative to that of the control cells cultured in a medium without polymers, followed the formula $[A]_{test}/[A]_{control} \times 100\%$, where $[A]_{test}$ and $[A]_{control}$ are the absorbance values of the wells (with the nanocomplexes) and control wells (only with pDNA), respectively. The cell viability of each sample was obtained from the measurement of six wells in parallel.

Scheme 1. Synthetic Processes of Bioreducible POSS-Based Gene Vectors via ATRP

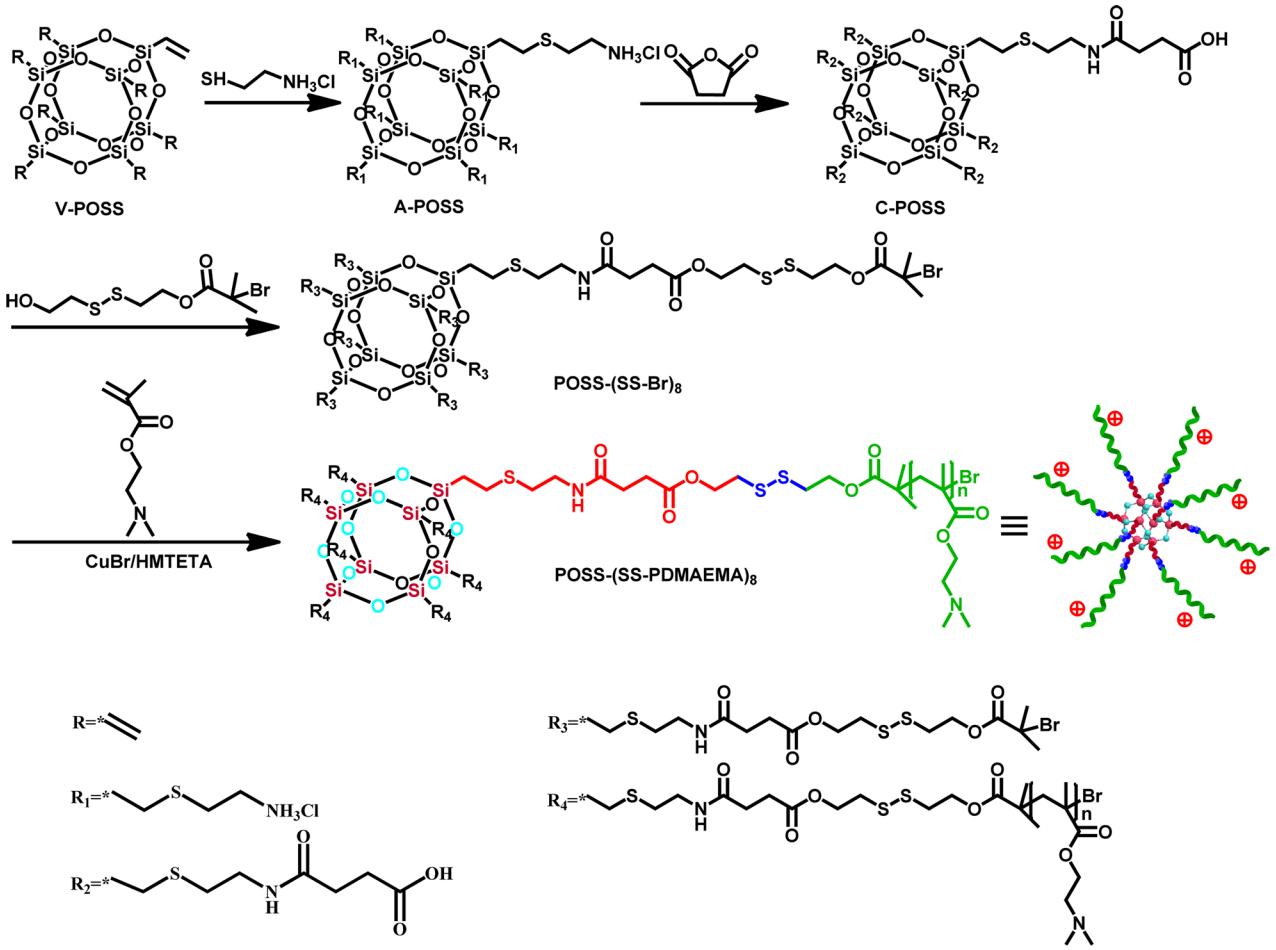

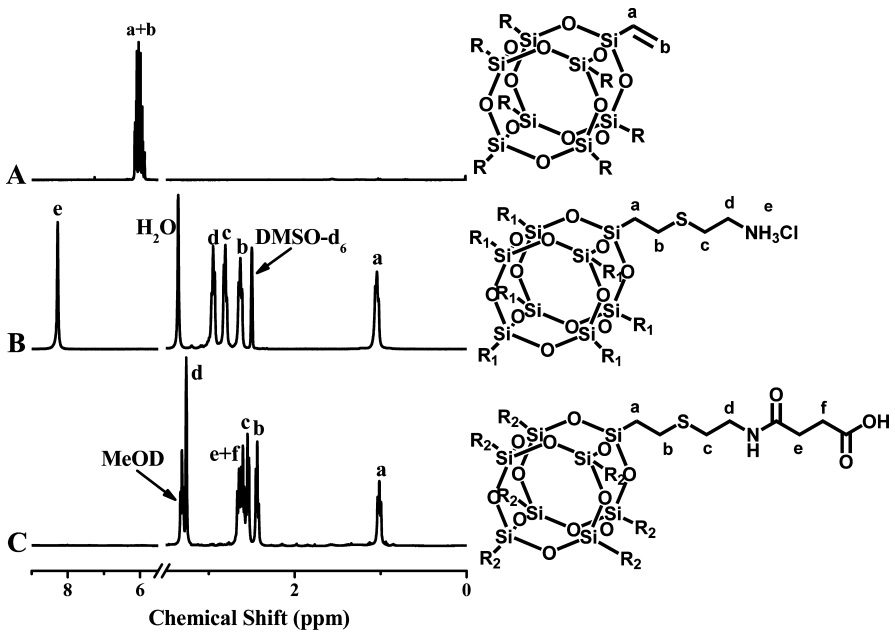

Figure 1. Typical ^{1}H NMR spectra of (A) V-POSS in $CDCl_3$, (B) A-POSS in DMSO-d_6, and (C) C-POSS in MeOD.

In Vitro Transfection Assay. The detailed procedure of transfection assay was reported in our earlier work.[30] Plasmid pRL-CMV and Enhanced green fluorescent protein (EGFP) pDNA (BD Biosciences, San Jose, CA) as reporter genes were used in transfection studies in vitro. The cells were cultured for 24 h before adding different N/P ratios polymer/pDNA nanocomplexes. After incubator for 4 h under standard incubator conditions, the medium was replaced with fresh culture medium and cells were incubated for another 20 h, resulting in a total

dx.doi.org/10.1021/am404585d | ACS Appl. Mater. Interfaces 2014, 6, 1044−1052

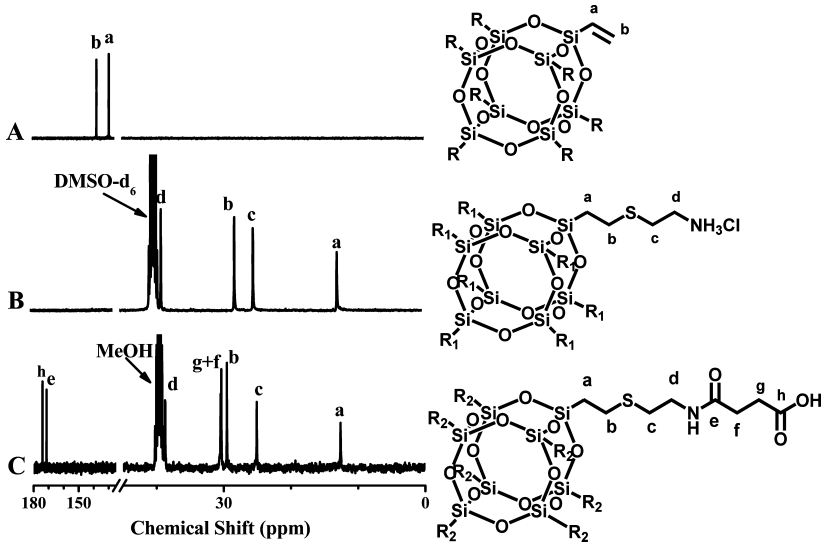

Figure 2. ^{13}C NMR spectra of (A) V-POSS in $CDCl_3$, (B) A-POSS in DMSO-d_6, and (C)C-POSS in DMSO-d_6.

transfection time of 24 h.[29] At the end of transfection, the cultured cells were washed with PBS and lysed with lysis reagent. Luciferase gene expression was quantified using a luminometer (Berthold Lumat LB 9507) and a commercial kit (Promega Co.). Bicinchoninic acid assay (Biorad Lab) was carried out to analyze the protein concentration in the cells. Results were expressed as relative light units (RLUs) per milligram of cell protein lysate (RLU/mg protein).

EGFP pDNA as another reporter gene was also used for gene delivery assay. The performance of the control POSS-$(PDMAEMA)_8$ and POSS-$(SS\text{-}PDMAEMA)_8$ counterpart was assessed in HepG2 (at N/P ratio of 20) and COS7 (at N/P ratio of 10) cell lines. The procedure was similar to those mentioned above. Leica DMIL Fluorescence Microscope and flow cytometry (FCM, Beckman Coulter) were applied to observe and measure the percentage of the transfected cells.

RESULTS AND DISCUSSION

Preparation of Bioreducible POSS-Containing Macro-ATRP Agents (POSS-$(SS\text{-}Br)_8$). It is significantly important to extend the length of arms on a V-POSS core for reducing steric hindrance and introducing eight bioreducible ATRP initiation sites completely. First, V-POSS was modified to be octa-substituted amine-terminated POSS (A-POSS) by click reaction. To further extend arm length, we used succinic anhydride to react with A-POSS, producing C-POSS with eight carboxyl acid groups. Disulfide-containing ATRP initiator, 2-bromo-2-methyl-propionic acid 2-(2-hydroxy-ethyldisulfanyl)-ethyl ester (BIBB-SS−OH), was introduced via esterification to obtain POSS-$(SS\text{-}Br)_8$ with eight biocleavable initiation sites. The process is summarized in Scheme 1.

A-POSS was synthesized by the method of "thiol−ene" click reaction. UV light motivated the reaction of A-POSS and cysteamine hydrochloride in the present of little amount DMAP as photoinitiator. Figure 1 reflected all vinyl groups of V-POSS were reacted with thiol groups. The peaks (a, b in Figure 1A) attributed to vinyl of V-POSS disappeared and the peaks of $-\underline{CH_2}-S-CH_2$ and $-CH_2-S-\underline{CH_2}-$ appeared at b and c in Figure 1B. ^{13}C NMR spectra also showed that all vinyl groups were modified to thioether bond in Figure 2A, B. The peaks (a, b in Figure 2A) attributed to vinyl of V-POSS shifted from ca. 128.50 and 137.18 ppm to ca. 12.74 and 27.93 ppm correspond to $Si-\underline{CH_2}-CH_2$ and $Si-CH_2-\underline{CH_2}$ in Figure 2B. Figure 3A and Figure 3B reflected that the peak position of silicon in V-POSS shifted from ca. −79.80 ppm to ca. −67.88 ppm. The one single

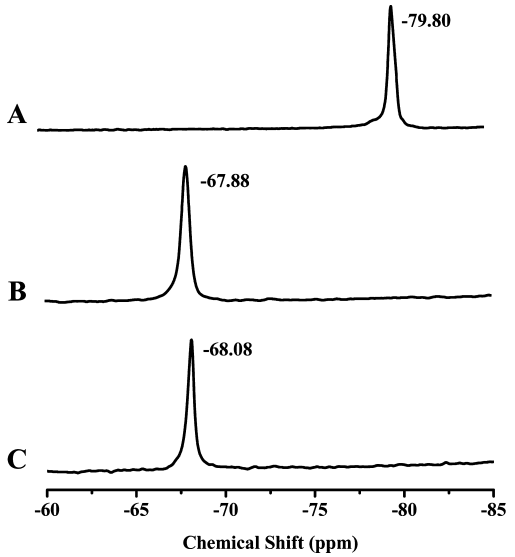

Figure 3. Typical ^{29}Si NMR spectra of (A) V-POSS in $CDCl_3$, (B) A-POSS in DMSO-d_6, and (C) C-POSS in DMSO-d_6.

sharp ^{29}Si NMR peak of A-POSS indicated that there was only one structural conformation of silicon atom in the compound. That was to demonstrate the A-POSS product was of the uniform structure and high purity. Compared with the traditional approach to synthesize POSS-$(NH_3Cl)_8$ through hydrolysis method,[33] this "thiol−ene" click method was easily operated and the byproducts were easily removed.

A-POSS was then modified to be C-POSS using succinic anhydride. ^1H NMR and ^{29}Si NMR confirmed that octa-substituted carboxyl-terminated POSS (C-POSS) possesses a perfect cagelike structure (Figures 1C, 2C, and 3C). The peak (d in Figure 1B) attributed to $-CH_2-\underline{CH_2}-NH_3Cl$ at ca. 2.95 ppm shifted to ca. 3.26 ppm corresponds to $-CH_2-\underline{CH_2}-NHCO$ in Figure 1C. The peak (e) at ca. 171.7 ppm ascribed to carbanyl group demonstrated that A-POSS was modified to C-POSS (Figure 2C). Panels B an C in Figure 3 reflected that the peak position of silicon in A-POSS shifted from ca. −67.88 ppm (Figure 3B) to ca. −68.08 ppm (Figure 3C), and the new peak was attributed to the silicon of C-POSS. The ^{29}Si NMR spectrum of C-POSS had

dx.doi.org/10.1021/am404585d | ACS Appl. Mater. Interfaces 2014, 6, 1044−1052

only one single sharp peak, indicating that there was only one structural conformation of silicon atom in C-POSS.

POSS-$(SS\text{-}Br)_8$ with eight initiation sites was synthesized by esterification reaction of C-POSS with BIBB-SS−OH. The integral area of methyl group, *k*, was triple of that of methylene group (a) adjacent to Si atom in Figure 4A, indicating that all of

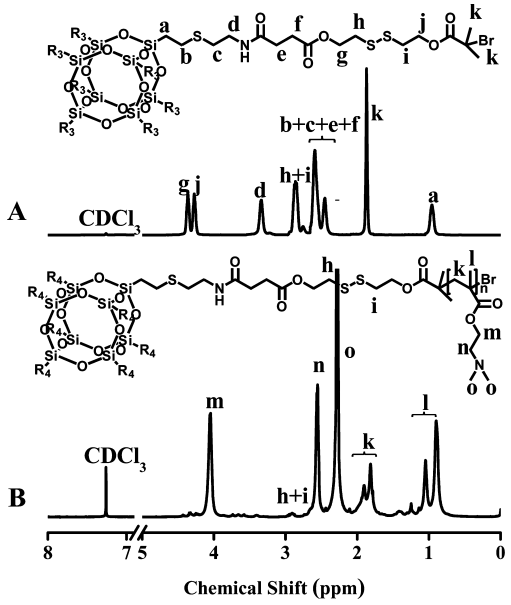

Figure 4. Typical ^1H NMR spectra of (A) POSS-$(SS\text{-}Br)_8$ and (B) POSS-$(SS\text{-}PDMAEMA2.3K)_8$ in $CDCl_3$.

eight organic corner groups were modified by BIBB-SS−OH. Figure 2C and Figure S2 (see the Supporting Information) showed that the ^{13}C NMR peak h attributed to carboxyl group of C-POSS shifted from ca. 174.1 ppm to ca. 171.4 ppm attributed to the carbanyl group in POSS-$(SS\text{-}Br)_8$. The disappearance of the peak of carboxyl group of C-POSS also indicated that eight ATRP sites of POSS-$(SS\text{-}Br)_8$ were successfully introduced.

Synthesis and Characterization of the POSS-$(SS\text{-}PDMAEMA)_8$s. Well-defined star-shaped POSS-$(SS\text{-}PDMAEMA)_8$s, consisting of a POSS core and eight bioreducible PDMAEMA arms, were synthesized via ATRP from the macroinitiator, POSS-$(SS\text{-}Br)_8$ (Scheme 1). By controlling the polymerization time, the length of PDMAEMA arms can be regulated to produce POSS-$(SS\text{-}PDMAEMA)_8$s with different molecular weight. The GPC results of POSS-$(SS\text{-}PDMAEMA)_8$s were summarized in Table 1. The M_n of POSS-$(SS\text{-}PDMAEMA)_8$s increased with extending reaction time from 20 to 40 min. The M_n vallues of 2.35×10^4, 2.90×10^4, and 3.43×10^4 g/mol corresponded to POSS-$(SS\text{-}PDMAEMA2.3K)_8$, POSS-$(SS\text{-}PDMAEMA3.1K)_8$ and POSS-$(SS\text{-}PDMAEMA3.8K)_8$. The number of DMAEMA repeat units per arm raised accordingly from 15 to 24, based on the assumption that POSS-$(SS\text{-}Br)_8$ possessed 8 ATRP initiation sites (Table 1). In addition, narrow molecular-weight distribution (polydispersity index (PDI), around 1.2) of POSS-$(SS\text{-}PDMAEMA)_8$s indicated that the ATRP processes of DMAEMA were well-controlled. Meanwhile, low PDI values of star-shaped polymers also showed that steric hindrance was negligible because the arm length of POSS-$(SS\text{-}Br)_8$ was long enough.

The typical chemical shifts associated with DMAEMA (repeat units) include peaks k (δ = 1.72−1.97 ppm, C−$\underline{CH_2}$), l (δ = 0.8−1.10 ppm, C−$\underline{CH_3}$), m (δ = 4.05 ppm, $\underline{CH_2}$−O−C═O), n (δ = 2.56 ppm, N−$\underline{CH_2}$) and o (δ = 2.27 ppm, N−$\underline{CH_3}$). The signal (h + i) of the POSS-$(SS\text{-}Br)_8$ became much lower because of the less contribution of POSS-$(SS\text{-}Br)_8$ to the overall structure of star-shaped polymers.

Table 1. Characterization of the Macro-ATRP Agent and Bioreducible Star-Shaped Cationic Polymers

sample	reaction time of ATRP (min)	M_n (g/mol)[c]	PDI[c]	monomer repeat units per arm[d]
POSS-$(SS\text{-}Br)_8$[a]		4.30×10^3	1.01	
POSS-$(SS\text{-}PDMAEMA2.3K)_8$[b]	20	2.35×10^4	1.20	15
POSS-$(SS\text{-}PDMAEMA3.1K)_8$[b]	30	2.90×10^4	1.23	20
POSS-$(SS\text{-}PDMAEMA3.8K)_8$[b]	40	3.43×10^4	1.20	24

[a]POSS-$(SS\text{-}Br)_8$ possesses eight ATRP initiation sites. [b]Synthesized using a molar feed ratio [DMAEMA (4 mL)]:[POSS-$(SS\text{-}Br)_8$]:[CuBr]:[HMTETA] of 120:0.125:1:1 at room temperature in 6 mL of methanol/water (5.9/0.1, v/v). [c]Determined from GPC results. PDI = weight average molecular weight/number average molecular weight, or M_w/M_n. [d]Determined from M_n and the molecular weights of POSS-$(SS\text{-}Br)_8$ (4.33×10^3 g/mol) and DMAEMA (157 g/mol).

The disulfide bridge linkages between POSS core and PDMAEMA arm chains will break down under reducible conditions and thus PDMAEMA arms fall off. To demonstrate the responsive ability, we exposed POSS-$(SS\text{-}PDMAEMA2.3K)_8$ to 10 mM of DL-dithiothreitol (DTT), analogous to the intracellular environment.[10] The GPC curves showed the degradation of the disulfide-linked POSS-$(SS\text{-}PDMAEMA2.3K)_8$ induced by DTT (Figure 5). It was clearly seen that the M_n of

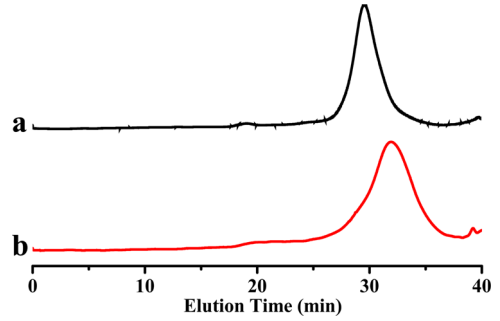

Figure 5. GPC traces of (a) POSS-$(SS\text{-}PDMAEMA2.3K)_8$ and (b) POSS-$(SS\text{-}PDMAEMA2.3K)_8$ in the presence of 10 mM DTT, where the incubation time was 1 h.

POSS-$(SS\text{-}PDMAEMA2.3K)_8$ declined substantially after treatment with DTT for 1 h. The PDI values increased from 1.20 to 1.52. The significant change after incubation with DTT explicitly implied that the POSS-$(SS\text{-}PDMAEMA)_8$s were sensitive under reducible condition.

In order to evaluate the effect of the disulfide linkages for gene delivery, we also synthesized the POSS-$(PDMAEMA)_8$ without disulfide linkages from the macroinitiator, POSS-Br_8. Their detailed procedure is illustrated in the Supporting Information. The total number of DMAEMA repeat units per arm of the control POSS-$(PDMAEMA)_8$ was 25 determined from M_n of 3.38×10^4 g/mol, which was similar to POSS-$(SS\text{-}PDMAEMA3.8K)_8$ with about 24 repeat units per arm. It was found that POSS-$(PDMAEMA)_8$ owned similar physiochemical

dx.doi.org/10.1021/am404585d | ACS Appl. Mater. Interfaces 2014, 6, 1044−1052

properties (except reducibility) to the POSS-(SS-PDMAEMA3.8K)$_8$ counterpart.

Biophysical Characterization of Polymer/pDNA Nanocomplexes. For an excellent gene delivery system, condensing pDNA into NPs (nanoparticles) small enough to facilitate cellular uptake was a prerequisite. Agarose gel electrophoresis, dynamic light scattering (DLS) and zeta potential measurements were utilized to confirm the ability of the star-shaped polycations to bind pDNA into NPs. Beyond those methods, AFM image was also used to observe the morphology of resultant NPs in the present work. First, agarose gel was used to prove the formation of the polymer/pDNA nanocomplexes at different N/P ratios. The gel retardation results of all nanocomplexes with increasing N/P ratios were demonstrated in Figure 6. All POSS-(SS-PDMAEMA)$_8$s and the control POSS-(PDMAEMA)$_8$ can bind pDNA completely at the N/P ratio of 1.5.

As mentioned earlier, disulfide bridge linkages possessed the responsivity under reducible conditions, which may have advantage on pDNA release from the nanocomplexes under intracellular reducible conditions. In the gel electrophoresis assay, when POSS-(SS-PDMAEMA2.3K)$_8$/pDNA nanocomplexes were exposed to reductive agent, DTT, the detached PDMAEMA arms still could hinder the migration of pDNA upon N/P ratio of 2 (Figure 6a′). Heparin[27,32] as a counter polyanion was introduced in this assay. When POSS-(SS-PDMAEMA2.3K)$_8$/pDNA nanocomplexes were exposed to heparin alone, pDNA was only released at the relative low N/P ratios (Figure 6a″). However, in the present of heparin and DTT, rapid pDNA release from the POSS-(SS-PDMAEMA2.3K)$_8$/pDNA nanocomplexes occurred at all tested N/P ratios (Figure 6a‴). Rapid pDNA release from POSS-(SS-PDMAEMA2.3K)$_8$/pDNA meant that unstable nanocomplexes were generated due to the cleavage of the PDMAEMA arm chains from the POSS core. Such unstable nanocomplexes led to fast decondensation through interchange with polycations. The resultant free pDNA migrated in the direction of the anode. In fact, kinds of cellular components including mRNA, nuclear chromatin and sulfated sugars can serve as destructors to induce pDNA release.[27] In company with GSH in cells, these destructors can promote the release of DNA, thus these bioreducible POSS-(SS-PDMAEMA)$_8$s may result in high transfection efficiency in vitro or in vivo.

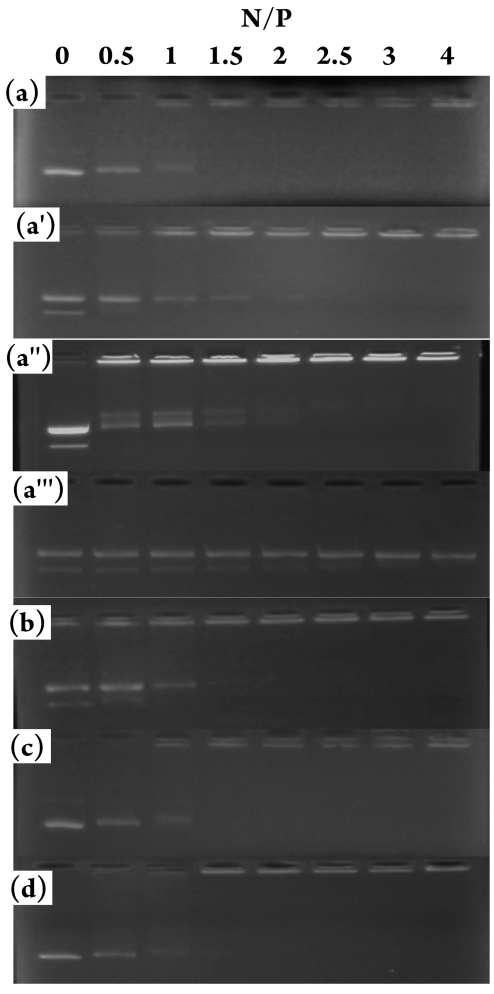

Figure 6. Electrophoretic mobility of pDNA in the nanocomplexes of the cationic polymers: (a) POSS-(SS-PDMAEMA2.3K)$_8$, (a′) POSS-(SS-PDMAEMA2.3K)$_8$ in the presence of 10 mM DTT, (a″) POSS-(SS-PDMAEMA2.3K)$_8$ in the presence of heparin as the counter polyanion, (a‴) POSS-(SS-PDMAEMA2.3K)$_8$ in the presence of 10 mM DTT and heparin where the incubation time was 30 min, (b) POSS-(SS-PDMAEMA3.1K)$_8$, (c) POSS-(SS-PDMAEMA3.8K)$_8$, and (d) POSS-(PDMAEMA)$_8$.

The particle size of nanocomplexes determined from DLS measurement could affect the behavior the endocytosis. NPs with diameters of less than 200 nm are less impressionable to clearance by the reticuloendothelial system (RES).[34] Figure 7A showed that all POSS-(SS-PDMAEMA)$_8$s can effectively bind DNA into NPs, and that the particle size decreased with the increasing of N/P ratio, which was similar to our earlier work.[10] At N/P ratio of 2.0, loose large NPs were generated because of the lower amount of cationic polymers. The diameter of all NPs was found to be stabilized in the range of 100−150 nm at higher N/P ratios. These NPs within this size range favor their cellular uptake.[34] The morphology of PDMAEMA2/pDNA nanocomplexes at N/P ratio of 10 was visualized in the AFM image (Figure 7C). The AFM image showed that POSS-(SS-PDMAEMA3.1K)$_8$ condensed pDNA into uniform NPs with the diameter of 100−200 nm, which was consistent with the result of DLS measurement (Figure 7A).

Zeta potential can scale the amount of surface charges on the polymer/pDNA NPs. It was also a significant factor affecting internalized behavior of the nanocomplexes. The surface charges of NPs were positive above the N/P ratio of 2 in Figure 7B. Electrostatic interaction between NPs with positively charges and negatively charged cell membranes facilitated endocytosis. Redundant star-shaped polycations had a weaker influence on particle size and zeta potential of the nanocomplexes at higher N/P ratios.

Cell Viability Assay. The cytotoxicity of gene carriers has a profound impact on the transfection efficiency for DNA delivery. Many factors may affect the cytotoxicity of gene vectors, such as molecular weight, polycation structure, charge density and bioreduction. In the present work, cytotoxicity of the polymer/pDNA nanocomplexes at different N/P ratios was estimated via MTT assay in HepG2 and COS7 cells (Figure 8). No obvious cytotoxicity was observed in this work, which was consistent with the earlier literature.[20,22,25,26] At higher N/P ratios, besides compact and positively charged nanocomplexes, there was also free polymer with positive charge in the transfection formulation. Excess of positive charge has damage to cells, which explained why cell viability presents downward trend with the increase of N/P ratios.

Cytotoxicity was also highly relevant with the arm length of star-shaped polymer. It was found that POSS-(SS-PDMAEMA3.8K)$_8$ with the longest PDMAEMA arms displayed highest

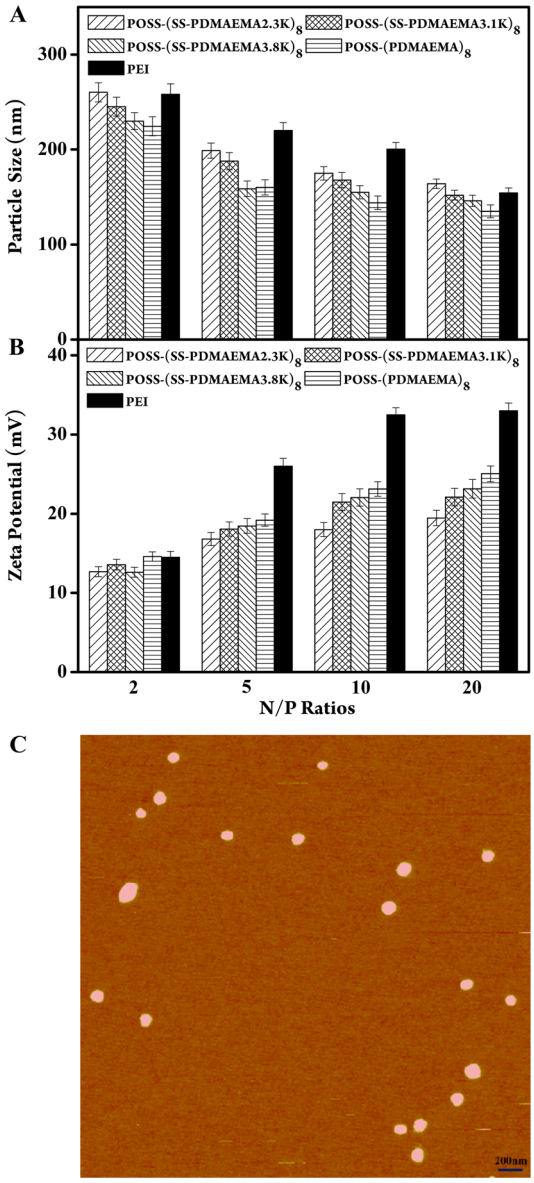

Figure 7. (A) Particle sizes and (B) zeta potentials of the nanocomplexes between the cationic polymers (POSS-(SS-PDMAEMA2.3K)$_8$, POSS-(SS-PDMAEMA3.1K)$_8$, POSS-(SS-PDMAEMA3.8K)$_8$, POSS-(PDMAEMA)$_8$ and PEI) and pDNA at different N/P ratios, and (C) AFM image of the POSS-(SS-PDMAEMA3.1K)$_8$/pDNA nanocomplexes at N/P of 10.

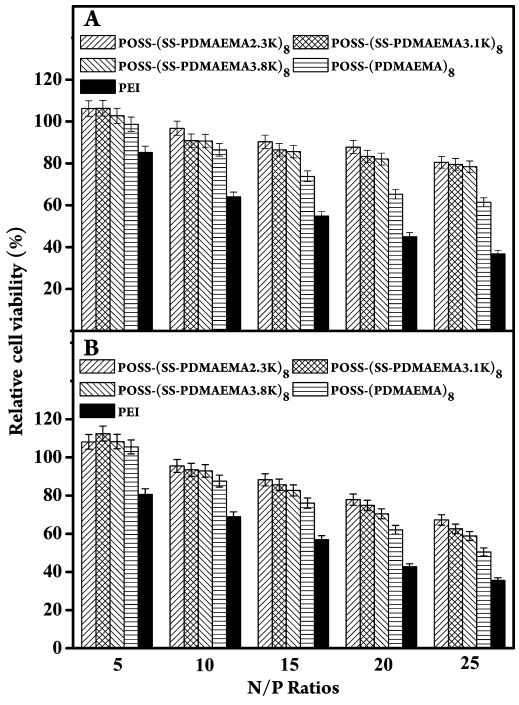

Figure 8. Cell viability of polymer/pDNA nanocomplexes at different N/P ratios in (A) HepG2 and (B) COS7 cell lines.

toxicity at all N/P ratio among the POSS-(SS-PDMAEMA)$_8$s. Cytotoxicity presented a rising trend with the increase of arm length, which was consistent with our earlier work.[10] Thus, controlling the cytotoxicity of POSS-(SS-PDMAEMA)$_8$s could be realized by adjustment of arm length of PDMAEMA.

The control POSS-(PDMAEMA)$_8$ had about 25 repeat units of DMAEMA per arm chain, similar to POSS-(SS-PDMAEMA3.8K)$_8$. However, the POSS-(PDMAEMA)$_8$/pDNA nanocomplexes displayed much higher cytotoxicity (Figure 8), indicating that the introduction of disulfide linkages can effectively reduce cytotoxicity of polymer/pDNA nanocomplexes. Polycations with high molecular weight can interact effectively with basic components (including the cell membrane, nucleic acid and proteins) in cells,[27] which negatively affected the survival of cells. However, POSS-(SS-PDMAEMA3.8K)$_8$ was readily degraded to be low-molecular-weight PDMAEMA arms and a biocompatible POSS core under the intracellular condition. PDMAEMA arms with lower molecular weight had lesser impact on cell survival and thus presented the lower cytotoxicity than POSS-(PDMAEMA)$_8$. It should be noted that in comparison with "gold-standard" PEI (25 kDa), the POSS-(PDMAEMA)$_8$/pDNA nanocomplexes exhibited much lower cytotoxicity because of its degradability.

In Vitro Gene Transfection Assay. Luciferase was first used as a gene reporter for assessing the in vitro gene transfection efficiency of star-shaped polycations in HepG2 cells and COS7 cells. Figure 9 showed the profile of luciferase expression mediated by POSS-(SS-PDMAEMA)$_8$s and POSS-(PDMAEMA)$_8$ at different N/P ratios in comparison with that of PEI (25 kDa) at the optimal N/P ratio[9] of 10 in complete serum media. It was found that gene transfection efficiency was greatly reliant on the N/P ratio of the nanocomplexes and arm length of the star-shaped polycations. With the increase in N/P ratio, the transfection efficiency of POSS-(SS-PDMAEMA)$_8$/pDNA nanocomplexes showed a trend of growth at the first stage, and then decreased slightly. At lower N/P ratios, polycations cannot effectively bind DNA and the resultant large-sized NPs enter cells with difficulty. At higher N/P ratios, free polycations generated in transfection formulation, and the amount of free polycations increases gradually with the increasing N/P ratios. The increasing cytotoxicity resulted from free polycations may lead to a decrease in transfection efficiency.

The transfection activity of POSS-(SS-PDMAEMA2.3K)$_8$ was much lower than those of other POSS-(SS-PDMAEMA)$_8$s in both cell lines, especially at lower N/P ratios. The relative high cytotoxicity of POSS-(SS-PDMAEMA3.8K)$_8$/pDNA at higher N/P ratios leaded to a substantial decrease in the transfection efficiency. Among the POSS-(SS-PDMAEMA)$_8$s, the POSS-(SS-PDMAEMA3.1K)$_8$/pDNA nanocomplexes exhibited the best transfection efficiency at the N/P ratio of 15. This observation demonstrated that the optimal transfection efficiency for the

dx.doi.org/10.1021/am404585d | ACS Appl. Mater. Interfaces 2014, 6, 1044−1052

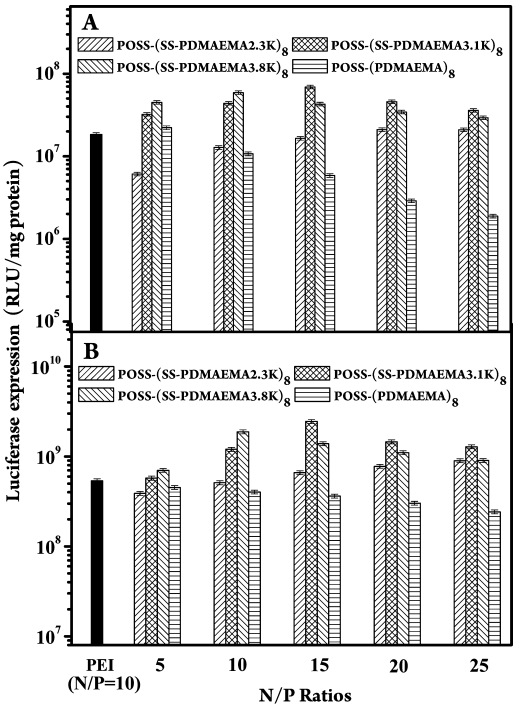

Figure 9. In vitro gene transfection efficiency of the cationic polymer/pDNA nanocomplexes at different N/P ratios in comparison with that of PEI (25KDa) (at the optimal N/P ratio of 10) in (A) HepG2 and (B) COS7 cell lines.

POSS-$(SS\text{-}PDMAEMA)_8$s was reliant on the suitable arm lengths of PDMAEMA. With the increase in the arm length of POSS-$(SS\text{-}PDMAEMA)_8$s, their optimal transfection efficiency generally rose first, followed by a slightly decline in both cell lines.

The gene transfection activity of POSS-$(SS\text{-}PDMAEMA3.8K)_8$ were much higher than those of the control POSS-$(PDMAEMA)_8$ at all N/P ratios in both cell lines (Figure 9). The transfection efficiency of POSS-$(SS\text{-}PDMAEMA3.8K)_8$/pDNA nanocomplexes could reach 12 times higher than that of POSS-$(PDMAEMA)_8$/pDNA nanocomplexes at N/P ratio of 20 in HepG2 cells. This result indicated that the existence of disulfide linkage in gene vector was significantly beneficial to gene delivery process. The POSS-$(SS\text{-}PDMAEMA3.8K)_8$/pDNA nanocomplexes became unstable under intracellular condition and then accelerated the pDNA release because of the responsivity of disulfide bridge linkages.

To intuitively verify the benefit of disulfide linkage to gene delivery systems, we adopted EGFP (enhanced green fluorescent protein) as another kind of gene reporter for gene transfection assay. In the present work, EGFP expression was examined by delivering the plasmid pEGFP-N1 encoding GFP in HepG2 and COS7 cell lines. As shown in Figure 9, the biggest difference in transfection efficiency mediated by POSS-$(SS\text{-}PDMAEMA3.8K)_8$ and POSS-$(PDMAEMA)_8$ at HepG2 cells and COS7 cells appeared at N/P ratio of 20 and N/P ratio of 10, respectively. Figure 10 displayed the typical images of EGFP expression mediated by POSS-$(SS\text{-}PDMAEMA3.8K)_8$ and POSS-$(PDMAEMA)_8$ in HepG2 cells (at the N/P ratio of 20) and COS7 cells (at the N/P ratio of 10). The fluorescence signal of POSS-$(SS\text{-}PDMAEMA3.8K)_8$/pEGFP delivery system were much stronger than that of POSS-$(PDMAEMA)_8$/pEGFP delivery system in the field of vision (Figure 10 and Figure S5 in the Supporting Information). The percentages of the EGFP-positive HepG2 cells were 28% for POSS-$(SS\text{-}PDMAEMA3.8K)_8$/pEGFP

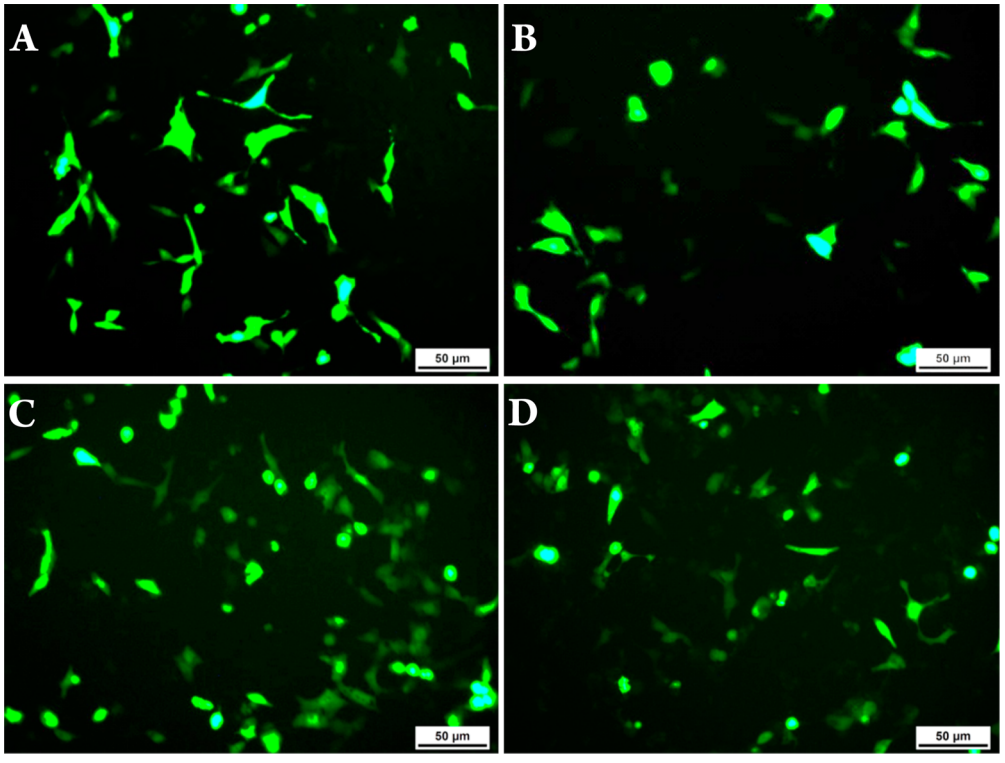

Figure 10. Images of EGFP expression mediated by (A) POSS-$(SS\text{-}PDMAEMA3.8K)_8$ and (B) POSS-$(PDMAEMA)_8$ at N/P ratio of 20 in HepG2 cells, (C) POSS-$(SS\text{-}PDMAEMA3.8K)_8$ and (D) POSS-$(PDMAEMA)_8$ at N/P ratio of 10 in COS7 cells. The percentages of the EGFP-positive HepG2 cells were 28 and 14%, and the percentages of the EGFP-positive COS7 cells were 36 and 25%, respectively, determined by flow cytometry.

dx.doi.org/10.1021/am404585d | ACS Appl. Mater. Interfaces 2014, 6, 1044−1052

and 14% for POSS-$(PDMAEMA)_8$/pEGFP, and the percentages of the EGFP-positive COS7 cells were 36% for POSS-(SS-PDMAEMA3.8K)$_8$/pEGFP and 25% for POSS-$(PDMAEMA)_8$/pEGFP respectively, determined by flow cytometry.[10] The above results also confirmed that POSS-$(SS\text{-}PDMAEMA)_8$ with disulfide bridges had much higher transfection activity than POSS-$(PDMAEMA)_8$ without disulfide linkages.

CONCLUSIONS

In summary, we demonstrated a facile way to synthesize a series of star-shaped gene carriers (POSS-$(SS\text{-}PDMAEMA)_8$s) via ATRP from a well-defined macro-ATRP agent, POSS-$(SS\text{-}Br)_8$. The POSS-$(SS\text{-}PDMAEMA)_8$s, consisting of a biocompatible POSS core, disulfide bridge and eight length-tailored PDMAEMA arms, showed excellent DNA condensation capacity, meanwhile the incorporation of disulfide bridge endowed the higher transfection activity and lower cytotoxicity than POSS-$(PDMAEMA)_8$ without disulfide bridge. Among these POSS-$(SS\text{-}PDMAEMA)_8$s, POSS-(SS-PDMAEMA3.1K)$_8$ exhibited the most excellent transfection performance at the N/P ratio of 15. These tailor-made bioreducible star-shaped polymers will be promising materials for gene therapy application.

ASSOCIATED CONTENT

Supporting Information

Preparation and characterization of BIBB-SS−OH, POSS-Br_8 and POSS-$(PDMAEMA)_8$. This material is available free of charge via the Internet at http://pubs.acs.org.

AUTHOR INFORMATION

Corresponding Authors

*E-mail: xufj@mail.buct.edu.cn.

*E-mail: dcwu@iccas.ac.cn.

Notes

The authors declare no competing financial interest.

ACKNOWLEDGMENTS

This work was supported by NSFC (Grants 21074007, 21174147, 51173014, 51103165, 51221002, and 51325304), Research Fund for the Doctoral Program of Higher Education of China (project number 20120010120007) and National "Young Thousand Talents Program".

REFERENCES

(1) Anderson, W. F. *Nature* **1998**, *392*, 25−30.
(2) Kershaw, M. H.; Westwood, J. A.; Darcy, P. K. *Nat. Rev. Cancer* **2013**, *13*, 525−541.
(3) Koirala, A.; Conley, S. M.; Naash, M. I. *Biomaterials* **2013**, *34*, 7158−7167.
(4) Fröhlich, T.; Wagner, E. *Soft Matter* **2010**, *6*, 226−234.
(5) Tian, H. Y.; Tang, Z. H.; Chen, X. S.; Jing, X. B. *Prog. Polym. Sci.* **2012**, *37*, 237−280.
(6) Ping, Y.; Wu, D. C.; Kumar, J. N.; Cheng, W. R.; Lay, C. L.; Liu, Y. *Biomacromolecules* **2013**, *14*, 2083−2094.
(7) Hu, H.; Xiu, K. M.; Xu, S. L.; Yang, W. T.; Xu, F. J. *Bioconjugate Chem.* **2013**, *24*, 968−978.
(8) Wang, H. Y.; Yi, W. J.; Qin, S. Y.; Li, C.; Zhuo, R. X.; Zhang, X. Z. *Biomaterials* **2012**, *33*, 8685−8694.
(9) Xu, F. J.; Zhang, Z. X.; Ping, Y.; Li, J.; Kang, E. T.; Neoh, K. G. *Biomacromolecules* **2009**, *10*, 285−293.
(10) Wang, Z. H.; Zhu, Y.; Chai, M. Y.; Yang, W. T.; Xu, F. J. *Biomaterials* **2012**, *33*, 1873−1883.
(11) Lin, C.; Blaauboer, C. J.; Timoneda, M. M.; Lok, M. C.; Steenbergen, M. V.; Hennink, W. E.; Zhong, Z. Y.; Feijen, J.; Engbersen, J. F. *J. Controlled Release* **2008**, *126*, 166−174.
(12) Luo, K.; Li, C. X.; Li, L.; She, W. C.; Wang, G.; Gu, Z. W. *Biomaterials* **2012**, *33*, 4917−4927.
(13) Wu, D. C.; Liu, Y.; Jiang, X.; He, C. B.; Goh, S. H.; Leong, K. W. *Biomacromulecules* **2006**, *7*, 1879−1883.
(14) Mao, S.; Sun, W.; Kissel, T. *Adv. Drug Delivery Rev.* **2010**, *62*, 12−27.
(15) Georgiou, T. K.; Vamvakaki, M.; Phylactou, L. A.; Patrickios, C. S. *Biomacromolecules* **2005**, *6*, 2990−2997.
(16) Hu, Y.; Zhu, Y.; Yang, W. T.; Xu, F. J. *ACS Appl. Mater. Interfaces* **2013**, *5*, 703−712.
(17) Zhu, Y.; Tang, G. P.; Xu, F. J. *ACS Appl. Mater. Interfaces* **2013**, *5*, 1840−1848.
(18) Plamper, F. A.; Schmalz, A.; Penott-Chang, E.; Drechsler, M.; Jusufi, A.; Ballauff, M.; Muller, A. H. E. *Macromolecules* **2007**, *40*, 5689−5697.
(19) Yin, M.; Ding, K.; Gropeanu, R. A.; Shen, J.; Berger, R.; Weil, T.; Mullen, K. *Biomacromolecules* **2008**, *9*, 3231−3238.
(20) Loh, X. J.; Zhang, Z. X.; Mya, K. Y.; Wu, Y. L.; He, C. B.; Li, J. *J. Mater. Chem.* **2010**, *20*, 10634−10642.
(21) He, C. B.; Wang, F. K.; Lu, X. H. *J. Mater. Chem.* **2011**, *21*, 2775−2782.
(22) Lu, Z. R.; Kaneshiro, T. L.; Wang, X. *Mol. Pharm.* **2007**, *4*, 759−768.
(23) Zhang, W. A.; Muller, A. H. E. *Prog. Polym. Sci.* **2013**, *38*, 1121−1162.
(24) Wang, X.; Li, D.; Yang, F.; Shen, H.; Li, Z. B.; Wu, D. C. *Polym. Chem.* **2013**, *4*, 4596−4600.
(25) Chen, M. H. *J. Dent. Res.* **2010**, *89*, 549−560.
(26) McCusker, C.; Carroll, J. B.; Rotello, V. M. *Chem. Commun.* **2005**, *41*, 996−998.
(27) Kang, H. C.; Kang, H. J.; Bae, Y. H. *Biomaterials* **2011**, *32*, 1193−1203.
(28) Wang, Y. H.; Zheng, M.; Meng, F. H.; Zhang, J.; Peng, R.; Zhong, Z. Y. *Biomacromolecules* **2011**, *12*, 1032−1040.
(29) Matyjaszewski, K.; Xia, J. H. *Chem. Rev.* **2001**, *101*, 2921−2990.
(30) Xu, F. J.; Li, H. Z.; Li, J.; Zhang, Z. X.; Kang, E. T.; Neoh, K. G. *Biomaterials* **2008**, *29*, 3023−3033.
(31) Bisht, H. S.; Manickam, D. S.; You, Y.; Oupicky, D. *Biomacromolecules* **2006**, *7*, 1169−1178.
(32) Lin, D. S.; Jiang, Q.; Cheng, Q.; Huang, Y. Y.; Huang, P. S.; Han, S. C.; Guo, S. T.; Liang, Z. C.; Dong, A. J. *Acta Biomater.* **2013**, *9*, 7746−7757.
(33) Tanaka, K.; Ishiguro, F.; Chujo, Y. *J. Am. Chem. Soc.* **2010**, *132*, 17649−17651.
(34) Nishiyama, N.; Kataoka, K. *Pharmacol.Ther.* **2006**, *112*, 630−648.